

## ■ Carbene Complexes | Hot Paper |

# Synthesis, Characterization, and Theoretical Investigation of Two-Coordinate Palladium(0) and Platinum(0) Complexes Utilizing $\pi$ -Accepting Carbenes

Sudipta Roy,<sup>[a]</sup> Kartik Chandra Mondal,<sup>[a]</sup> Jann Meyer,<sup>[a]</sup> Benedikt Niepötter,<sup>[a]</sup> Christian Köhler,<sup>[a]</sup> Regine Herbst-Irmer,<sup>[a]</sup> Dietmar Stalke,<sup>\*[a]</sup> Birger Dittrich,<sup>[b]</sup> Diego M. Andrada,<sup>[c]</sup> Gernot Frenking,<sup>\*[c]</sup> and Herbert W. Roesky<sup>\*[a]</sup>

Dedicated to Professor Spyros P. Perlepes on the occasion of his 60th birthday

**Abstract:** An elegant general synthesis route for the preparation of two coordinate palladium(0) and platinum(0) complexes was developed by reacting commercially available tetrakis(triphenylphosphine)palladium/platinum with  $\pi$ -accepting cyclic alkyl(amino) carbenes (cAACs). The complexes are characterized by NMR spectroscopy, mass spectrometry, and single-crystal X-ray diffraction. The palladium complexes exhibit sharp color changes (craylochromism) from dark maroon to bright green if the C-Pd-C bond angle is sharpened by approximately  $6^\circ$ , which is chemically feasible by elimination of one lattice THF solvent molecule. The analogous dark orange-colored platinum complexes are more rigid and thus do not show this phenomenon. Additionally,  $[(cAAC)_2Pd/Pt]$  complexes can be quasi-reversibly oxidized to their corresponding  $[(cAAC)_2Pd/Pt]^{+}$  cations, as evidenced by cyclic voltammetry measurements. The bonding and stability are studied by theoretical calculations.

Since the first report of stable N-heterocyclic carbenes (NHCs) in 1991,<sup>[1]</sup> they have been utilized for the stabilization of unusual species over the past two and a half decades.<sup>[2]</sup> NHCs are chosen as superior  $\sigma$ -donors and employed as ligands in different fields of chemistry.<sup>[1,2]</sup> The carbene carbon atom of an NHC

is bonded to two  $\sigma$ -withdrawing and  $\pi$ -donating nitrogen atoms.<sup>[2a]</sup> Consequently, the accumulation of electron density on the  $p_z$  orbital of the carbene atom is reasonably high, leading to weak  $\pi$ -accepting properties.<sup>[2e]</sup> This has both advantages and disadvantages with regards to the stabilization and isolation of unusual chemical species.<sup>[3]</sup> The strong  $\sigma$ -donation ability of NHCs has been utilized for the stabilization and characterization of numerous unusual species, whereas the weaker  $\pi$ -accepting property makes NHC-containing compounds more labile.<sup>[4]</sup> As a result, they are prone to decomposition and hence, are less suitable for characterization by mass spectrometry. Since the synthetic reports of cyclic alkyl(amino) carbenes (cAACs) a decade ago,<sup>[5]</sup> they have been utilized as superior ligands for the stabilization of unstable chemical species,<sup>[6]</sup> radicals,<sup>[7]</sup> and elements in their different oxidation states<sup>[8]</sup> due to their stronger  $\pi$ -accepting properties. One  $\sigma$ -withdrawing and  $\pi$ -donating nitrogen atom of an NHC is replaced by a  $\sigma$ -donating quaternary carbon atom in cAAC leading to a lower lying LUMO. This is energetically advantageous for acceptance of  $\pi$  back-donation from the element bound to the carbene carbon atom of cAAC.<sup>[9]</sup> Experimental results suggest that the carbene carbon atom of cAAC utilizes the lone pair of electrons on the adjacent nitrogen atom in a more controlled way, depending on the accumulation of electron density on the elements that are bound to the cAAC.<sup>[5–8]</sup> cAACs form stronger donor-acceptor bonds which provide better stability in the systems.<sup>[10]</sup> Structural bond parameters and theoretical investigations of cAAC-containing chemical species unravel the hidden potential of cAACs and their ability to control the distribution of electron densities around the bound element. This is strongly reflected in the C–N bond length, which varies in the range of 1.30 to 1.42 Å depending on the elements bound and their oxidation states.<sup>[5–10]</sup>

Since the first synthesis report of an NHC, only  $[(NHC)_2Ni]$ ,  $[(NHC)_2Pd]$ , and  $[(NHC)_2Pt]$  complexes with zero oxidation state and a coordination number of two have been reported.<sup>[11]</sup> Very recently, cAAC-stabilized first-row transition metal atoms ( $[(cAAC)_2M]$ ; M = Mn, Fe, Co, Ni, Cu, Zn) have been reported,<sup>[12]</sup> with formal oxidation states of zero, one, or two and low coordination numbers, which has not been achieved with NHC ligands. Structural parameters and bonding investigations of these neutral  $[(cAAC)_2M]$  complexes showed very different

[a] Dr. S. Roy, Dr. K. C. Mondal, Dipl.-Chem. J. Meyer, Dipl.-Chem. B. Niepötter, C. Köhler, Dr. R. Herbst-Irmer, Prof. Dr. D. Stalke, Prof. Dr. H. W. Roesky  
Institut für Anorganische Chemie, Georg-August-Universität  
Tammannstrasse 4, 37077-Göttingen (Germany)  
E-mail: dstalke@chemie.uni-goettingen.de  
hroesky@gwdg.de

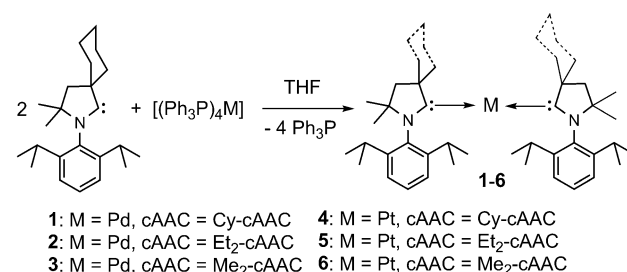
[b] Dr. B. Dittrich  
Institut für Anorganische und Angewandte Chemie, Universität Hamburg  
Martin-Luther-King-Platz 6, Raum AC 15c (Erdgeschoss)  
20146 Hamburg (Germany)

[c] Dr. D. M. Andrada, Prof. Dr. G. Frenking  
Fachbereich Chemie, Philipps-Universität Marburg  
Hans-Meerwein-Strasse 35032 Marburg (Germany)  
E-mail: frenking@chemie.uni-marburg.de

Supporting information for this article is available on the WWW under <http://dx.doi.org/10.1002/chem.201500758>, including synthetic procedures for complexes 1–6 and crystal structure determination for 1-THF, 1, 3-0.5 THF, 4-THF, 5-0.5 THF, and 6-0.5 THF.

electronic situations for different metals (see the Supporting Information, Figure S1). Note, that the EPR spectroscopy and theoretical investigations unambiguously conclude that Mn<sup>[12a]</sup> and Cu<sup>[12e]</sup> mostly prefer the formal oxidation state one in [(cAAC)<sub>2</sub>Mn] and [(cAAC)<sub>2</sub>Cu], respectively. Both of these complexes have a delocalized radical electron spanning over the two carbene carbon atoms. However, the complex [(cAAC)<sub>2</sub>Zn] favors a diradicaloid singlet spin ground state with Zn in the formal oxidation state two.<sup>[12f]</sup> In contrast, there is strong  $\pi$ -back-donation from Fe<sup>0</sup>, Co<sup>0</sup>, and Ni<sup>0</sup><sup>[12b-d]</sup> to the carbene carbon atoms in [(cAAC)<sub>2</sub>Fe] ( $d^8$ ), [(cAAC)<sub>2</sub>Co] ( $d^9$ ), and [(cAAC)<sub>2</sub>Ni] ( $d^{10}$ ) complexes without a delocalized radical electron on carbenes (Figure S1). The electronics of the [(cAAC)<sub>2</sub>M] complexes are apparently unpredictable without experimental evidence and theoretical calculations. The electronics of second- or third-row two-coordinate [(cAAC)<sub>2</sub>M] complexes are intriguing. Analogous [(cAAC)<sub>2</sub>M] complexes with second-row transition metals have not been reported to date, whereas, among cAAC–third-row transition-metal(0) complexes, only two-coordinate [(cAAC)<sub>2</sub>Au] was synthesized and its bonding was theoretically investigated.<sup>[13a]</sup> The electronic structures of transition metal complexes [(cAAC)<sub>2</sub>M] were accurately predicted by different levels of theoretical investigations, since the C–N bond length does not always confirm the presence of the desired radical electron on the carbene carbon atom.<sup>[12,13a]</sup> Carbene metal complexes often act as catalysts and hence they are very important species. Additionally,  $\pi$ -accepting ligands are suggested to be advantageous since they can stabilize intermediate monoligated metal(0) complexes for amination and coupling reactions.<sup>[13b,c]</sup> Herein, we report on the synthesis, characterization, and theoretical calculation of [(cAAC)<sub>2</sub>Pd<sup>0</sup>] (**1–3**) and [(cAAC)<sub>2</sub>Pt<sup>0</sup>] (**4–6**) complexes (Scheme 1) with two-coordinate palladium and platinum, respectively.

Cy–cAAC and [(Ph<sub>3</sub>P)<sub>4</sub>Pd] were dissolved in 11:2 molar ratio in THF, forming a dark green solution of [(Cy–cAAC)<sub>2</sub>Pd] (**1**) which was stirred at room temperature (RT) for 1 h then 20 min at 70 °C and finally a further 12 h at RT. A similar synthetic method was used for the preparation of [(Et<sub>2</sub>–cAAC)<sub>2</sub>Pd] (**2**). The least sterically crowded carbene [(Me<sub>2</sub>–cAAC)] was found to be the most reactive one among these three ligands and was required only in 4.5 equiv to that of [(Ph<sub>3</sub>P)<sub>4</sub>Pd] to produce the dark maroon needles of [(Me<sub>2</sub>–cAAC)<sub>2</sub>Pd]·0.5 THF (**3**·0.5 THF). The yields of complexes (cAAC)<sub>2</sub>Pd<sup>0</sup> (**1–3**) largely depend on the molar ratio of cAAC and (Ph<sub>3</sub>P)<sub>4</sub>Pd. When the reaction was performed with a 2:1 molar ratio, unreacted [(Ph<sub>3</sub>P)<sub>4</sub>Pd] crystallized along with the product [(cAAC)<sub>2</sub>Pd<sup>0</sup>]. Use of the less bulky [Me<sub>2</sub>–cAAC] ligand led to a faster reaction and higher yield (90% for **3**·0.5 THF). The yield was little lower (85% for **2** and 84% for **1**) for relatively more bulky carbenes, Et<sub>2</sub>–cAAC or Cy–cAAC, and longer times are required for completion of the reaction (see the Supporting Information for details). To obtain the above-mentioned yields, the cAAC/[(Ph<sub>3</sub>P)<sub>4</sub>Pd] molar ratios were optimized to 11:2, 5:1, and 9:2 for **1**, **2**, and **3**·0.5 THF, respectively.



Scheme 1. Synthesis of complexes **1–6**.

The dark green solution of **1** was stored at –32 °C from which dark maroon rods of complex **1**·THF were formed in 84% yield. **1**·THF was characterized by single-crystal X-ray diffraction. When the crystals of **1**·THF were separated by filtration, interestingly the maroon rods immediately turned to bright green powder. The transformation from crystals to powder suggests the loss of lattice solvent (THF) but the reason behind such an immediate and dramatic change of color was not understood initially. When the green powder of **1** was redissolved in THF, it produced a green solution and recrystallization from THF or toluene at room temperature resulted in small green crystals. Single-crystal X-ray diffraction on the green crystal showed a similar molecular structure to that of complex **1**, albeit without any lattice solvent molecules. The structural deformation might be caused by the interfering solvent molecule. Indeed, a change in the C–Pd–C angle was observed (172.75° to 166.94°; Table 1). Replacing the Cy–cAAC

Table 1. Selected bond lengths [ $\text{\AA}$ ], bond angles [ $^\circ$ ] and colors of (Cy–cAAC)<sub>2</sub>Pd·THF (**1**·THF) and (Cy–cAAC)<sub>2</sub>Pd (**1**).

Complex	<b>1</b> ·THF	<b>1</b>
color	dark maroon	bright green
Pd1–C <sub>cAAC</sub> [ $\text{\AA}$ ]	2.0230(15)/2.0184(15)	2.0019(15)/2.0051(15)
C <sub>cAAC</sub> –N1 [ $\text{\AA}$ ]	1.3267(18)/1.3341(19)	1.3216(18)/1.3204(19)
C <sub>cAAC</sub> –Pd1–C <sub>cAAC</sub> [ $^\circ$ ]	172.75(6)	166.94(6)
N1–C <sub>cAAC</sub> –C2 [ $^\circ$ ]	106.57(12)/106.95(12)	107.03(3)/107.0(3)
N1–C <sub>cAAC</sub> –Pd1 [ $^\circ$ ]	130.08(11)/130.44(11)	133.15(11)/131.81(11)
C2–C <sub>cAAC</sub> –Pd1 [ $^\circ$ ]	123.25(10)/122.60(10)	119.7(3)/121.0(3)
sum of angles around C <sub>cAAC</sub> [ $^\circ$ ]	360	360
sum of angles around N1 [ $^\circ$ ]	360	360
adopted geometry of C <sub>cAAC</sub>	trigonal planar	trigonal planar
adopted geometry of Pd1	bent	bent

ligand with Et<sub>2</sub>–cAAC always led to similar green crystals of nonsolvated **2** and the color of the crystals did not depend on the temperature of crystallization. The replacement of Cy–cAAC or Et<sub>2</sub>–cAAC by the comparatively less bulky Me<sub>2</sub>–cAAC always produced dark maroon rods of **3**·0.5 THF, independent of the imposed temperature of crystallization. **3**·0.5 THF does not lose its lattice solvent and hence retains its color even after separation from the mother liquor. These observations all clearly suggest that employment of less bulky cAACs leads to wider C–Pd–C angles (171.26 for **3**·0.5 THF). The comparatively

more bulky carbene forms a complex with a smaller C-Pd-C ( $166.94^\circ$  for **1**) bond angle at room temperature under identical crystallization conditions. When the round-bottom flask containing a solution of **1**-THF is viewed from below, the solution looks greenish at the edge with a dominant maroon color in the middle. A change of the solvent from THF to toluene or benzene did not produce a different color, indicating that this color change is due to slight changes in the crystal structure of the carbene–metal chromophores. This crystallochromism/vapochromism effect is clearly resolved in **1**/1-THF. To our knowledge, no carbene–metal(0) complexes have to date been known to exhibit such phenomena. The previously reported  $[(\text{NHC})_2\text{Pd}]$  complexes are mostly yellow in color,<sup>[11b,14]</sup> indicating that the  $\pi$ -accepting cAAC has a strong effect on the complexes' energy levels, which are responsible for their corresponding electronic transitions.

Two-coordinate  $[(\text{NHC})_2\text{Pt}^0]$  complexes<sup>[11a,15]</sup> have rarely been synthesized and characterized, whereas their  $\pi$ -accepting cAAC analogues are not known. When cAAC was added to a light yellow solution of  $[(\text{Ph}_3\text{P})_4\text{Pt}]$  in 1:5 molar ratio at room temperature, the color of the reaction mixture slowly turned to light orange after 30 min, indicating the formation of the desired  $[(\text{cAAC})_2\text{Pt}]$  product.  $^{31}\text{P}$  NMR spectroscopy showed that the reaction was indeed slow. The reaction was found to be accelerated and completed in a few hours (3.5 h) when the reaction solution was boiled. Dark orange solutions of  $[(\text{cAAC})_2\text{Pt}^0]$  complexes [cAAC = Cy–cAAC (**4**), Et<sub>2</sub>–cAAC (**5**), Me<sub>2</sub>–cAAC (**6**)] were concentrated and stored in a freezer at  $-32^\circ\text{C}$  to form orange block crystals of **4**-THF, **5**·0.5THF, and **6**·0.5THF in 68, 74, and 79% yields, respectively.

The red rods/blocks of complexes **1**–**6** are stable in air for several hours and then slowly turn to red-brown solids within a day (Pd; **1**–**3**) or several days (Pt; **4**–**6**), but are stable for several months under an inert atmosphere at RT. Complexes **1** and **3** decompose above  $230^\circ\text{C}$  and **4**, and **6** above  $205^\circ\text{C}$ , whereas **2** and **5** decompose at  $170^\circ\text{C}$  and  $145^\circ\text{C}$ , respectively. The UV/Vis absorption spectra of **1**, **2**, and **3** show four absorption bands in the visible range (421/413/418, 466/461/464, 598/590/588, and 695/675/683 nm), whereas the orange-colored platinum analogues **4**, **5**, and **6** exhibit the corresponding bands at 452/450/449 nm (see the Supporting Information). Complexes **1** ( $m/z$  756.4 [ $M^+$ ]), **2** ( $m/z$  732.4 [ $M^+$ ]), **3** ( $m/z$  678.4 [ $M^+$ ]), **4** ( $m/z$  845.5 [ $M^+$ ]), **5** ( $m/z$  821.5 [ $M^+$ ]), and **6** ( $m/z$  765.4 [ $M^+$ ]) were characterized by electron-ionization mass spectrometry. Note that  $\{(\text{cAAC})\text{Pd}\}$  (previously proposed<sup>[13b,c]</sup> monoligated palladium) fragments are clearly observed for all three  $[(\text{cAAC})_2\text{Pd}]$  complexes (**1**–**3**; see the Supporting Information).

Single-crystal X-ray structure determination of the  $[(\text{cAAC})_2\text{M}]$  complexes ( $\text{M}=\text{Pd}$ , **1**/1-THF, **3**·0.5THF;  $\text{M}=\text{Pt}$ , **4**-THF, **5**·0.5THF and **6**·0.5THF) showed similar molecular structures. The structural aspects of **1**/1-THF and **6**·0.5THF are described herein (for **3**·0.5THF, **4**-THF, and **5**·0.5THF, see the Supporting Information). Complex **1** crystallizes in the triclinic  $P\bar{1}$  system with a lattice solvent molecule (THF) as **1**-THF and in the monoclinic space group  $P2_1/n$  without any lattice solvent molecule (Figure 1). In both cases, only one molecule is present in the asymmetric unit.

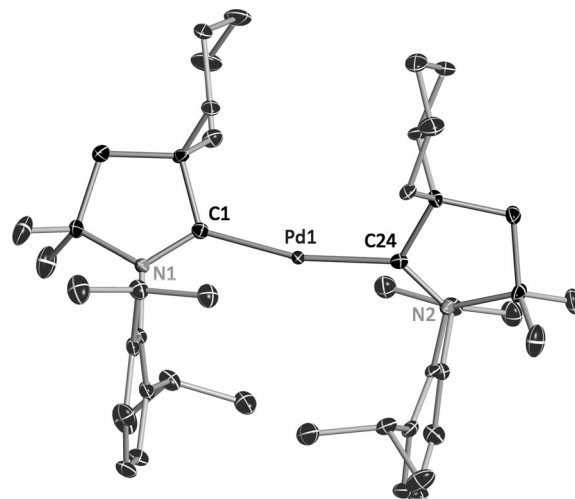


**Figure 1.** The molecular structure of complex **1**. H atoms are omitted for clarity. Anisotropic displacement parameters are depicted at the 50% probability level. Selected experimental [calculated at M06/def2-SVP] bond lengths [ $\text{\AA}$ ] and angles [ $^\circ$ ]: C1–Pd1 2.0019(15) [2.040], C24–Pd1 2.0051(15) [2.040], C1–N1 1.3216(18) [1.326], C24–N2 1.3204(19) [1.326], C1–Pd1–C24 166.94(6) [170.3].

The central palladium atoms adopt a slightly bent geometry with C–Pd–C bond angles ( $172.75(6)^\circ$  in **1**-THF and  $166.94(6)^\circ$  in **1**) that are smaller than those of  $[({}^{\text{ad}}\text{NHC})_2\text{Pd}]$  ( $180^\circ$ ;  ${}^{\text{ad}}\text{NHC}$  = 1,3-bisadamantylimidazolin-2-ylidene).<sup>[11b]</sup> Previously reported  $[\text{Pd}(\text{CNAr}^{\text{Dipp}_2})_2]$  ( $\text{Ar}^{\text{Dipp}_2}$  = 2,6-(2,6-*i*Pr<sub>2</sub>C<sub>6</sub>H<sub>3</sub>)<sub>2</sub>C<sub>6</sub>H<sub>3</sub>), stabilized by  $\pi$ -accepting aryl isocyanide, features a C–Pd–C bond angle of  $169.8(2)^\circ$ . The C–Pd distances of **1**/1-THF (2.0019(15)–2.0230(15)  $\text{\AA}$ ) are close to those of previously reported  $[({}^{\text{ad}}\text{NHC})_2\text{Pd}]$  (ca. 2.07–2.08  $\text{\AA}$ ). The C<sub>carbene</sub>–N bond lengths in **1**/1-THF are between 1.3204(19) and 1.3341(19)  $\text{\AA}$ , which are slightly longer than that of the related free carbene (ca. 1.30  $\text{\AA}$ ),<sup>[5]</sup> indicating  $\pi$  back-donation from Pd to the carbene carbon atoms. The superposition of related molecules of **1** and **1**-THF shows the distortions in the five-membered carbene ring and cyclohexyl aliphatic part of Cy–cAAC units (see the Supporting Information). The slight changes in the carbene–Pd unit lead to the dramatic shift in color (dark maroon for **1**-THF to bright green for **1**) of the same complex. Selected bond lengths and angles of **1**-THF and **1** are given in Table 1.

Complex  $[(\text{Me}_2\text{–cAAC})_2\text{Pt}]\cdot 0.5\text{THF}$  (**6**·0.5THF) crystallizes in the triclinic  $P\bar{1}$  space group with half of a lattice solvent molecule in the asymmetric unit (0.5THF). The central platinum atom is coordinated by two Me<sub>2</sub>–cAAC carbenes to adopt a linear geometry (Figure 2) with a C–Pt–C bond angle of  $170.9(2)^\circ$ , which is close to that of  $[(\text{Cy–cAAC})_2\text{Pt}]\cdot \text{THF}$  (ca.  $172.75(6)^\circ$ ). The C–Pt distances are 1.964(5) and 1.967(5)  $\text{\AA}$ . The C–N bonds (1.339(7)–1.345(6)  $\text{\AA}$ ) are slightly longer than those in **1**/1-THF (see Table 1), suggesting a stronger back-donation from Pt to the carbene carbon atoms. The bond lengths and angles are close to those values previously reported for  $[(\text{NHC})_2\text{Pt}^0]$ .<sup>[11a,15]</sup>

A general trend has been observed. Complexes (cAAC)<sub>2</sub>Zn, (cAAC)<sub>2</sub>Mn and (cAAC)<sub>2</sub>Cu have two Dipp groups on the oppo-

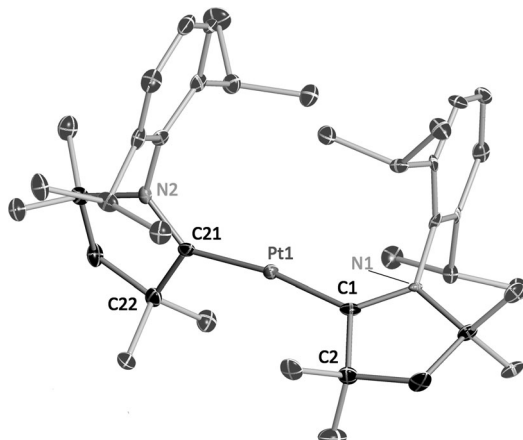


**Figure 2.** Molecular structure of **6**-0.5 THF. H atoms are omitted for clarity. Anisotropic displacement parameters are depicted at the 50% probability level. Selected experimental [calculated for **6** at M06/def2-SVP] bond lengths [Å] and angles [°]: C1–Pt1 1.964(5) [2.014], C21–Pt1 1.967(5) [2.014], C1–N1 1.339(7) [1.332], C21–N2 1.345(6) [1.332]; C1–Pt1–C21 170.9(2) [172.7].

site side with respect to the metal center ( $M=Zn, Cu, Mn$ ). In these complexes the radical electron is on the carbene carbon atoms.<sup>[12a,e,f]</sup> In contrast,  $(cAAC)_2Fe$ ,  $(cAAC)_2Co$ ,  $(cAAC)_2Ni$ ,  $(cAAC)_2Pd$  and  $(cAAC)_2Pt$  complexes have two Dipp groups on the same side. There are strong  $\pi$  back-donations from metal to carbene carbon atoms which might be a possible reason ( $M=Fe, Co, Ni, Pd, Pt$ ). Note, that there is no radical electron on the carbene carbon atom for  $M=Fe, Co, Ni, Pd, Pt$ . The orientation of two cAACs in  $(cAAC)_2M$  has huge effect on the spin ground state and fine electronic structure. Previously, we have realized that if two cAAC groups are in  $(cAAC)_2Ni$  similarly oriented like in  $(cAAC)_2Mn$  (e.g., on the same side), then there will be two radical electrons on the carbene carbon atoms, for example,  $(cAAC)_2Ni$ , which is not the spin ground state but rather an excited state. This was concluded from ab initio calculations (see the Supporting Information of ref. [12]).

We performed DFT calculations<sup>[16]</sup> on complexes **1**, **3**, and **6** to gain insight into the electronic structure. The most important bond lengths and angles of the optimized structures are given in Figures 1, 2, and S13 (see the Supporting Information). The theoretical and experimental data are in good agreement. The calculated Pd–C and Pt–C distances are slightly longer than the experimental values, which is a feature commonly observed between solid-state and theoretical structures.<sup>[17]</sup> In all the complexes the angle C1–M–C24 is close to 170°, namely, 170.3°, 171.9° and 172.7° for **1**, **3** and **6**, respectively. It is interesting to note that the theoretical C1–M–C24 angle in **1** is in better agreement with the experimental value of the **1**–THF crystal structure than with the value for pure **1** (Table 1). This supports the idea of the role of the THF solvent molecule in disturbing the intermolecular forces within the lattice of **1**. The bending potential is very shallow. The energy necessary to reduce the size of the C1–M–C24 angle from 172 to 166° was computed to be only 0.5 kcal mol<sup>-1</sup>.

To interpret the UV/Vis spectra, we carried out TD-DFT calculations in the gas phase and in THF solution (PCM model) at

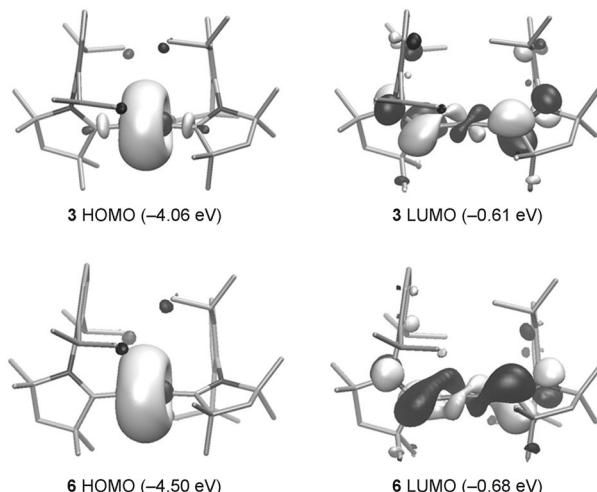


**Figure 3.** The HOMO and LUMO of complex **3** and **6** at M06/def2-TZVPP//M06/def2-SVP.

the M06/def2-TZVPP level of theory for **3** and **6** (see the Supporting Information, Tables S11–S13). The calculations in the gas phase reveal the occurrence of four main excitations, namely, HOMO→LUMO (590.4/514.5 nm for **3/6**), HOMO→LUMO+1 (507.0/444.9 nm), HOMO→LUMO+2 (413.5/360.7 nm), and HOMO→LUMO+3 (403.9/354.2 nm), which are in close agreement with the experimental data. Figure 3 shows the shape of the HOMO and LUMO of **3** and **6**. The HOMO is fully located on the transition metal, whereas the LUMO is located on the carbene ligands. By considering the solvent, the wavelength of the absorption is blue shifted by approximately 30 nm, due to the higher stabilization of the HOMO (see the Supporting Information, Figure S16) and the slightly stronger oscillator strength. We studied the variation of the spectrum of **3** with changes in the angle C1–M–C24. Results show that on going from 160° to 175° the main excitations shift to longer wavelengths and the oscillator strength values become higher.

We also investigated the bonding in the complexes by using the Natural Bond Orbital (NBO) and Energy Decomposition Analysis (EDA) methods.<sup>[18]</sup> The EDA has proven to give important information about the nature of the bonding. In this method, the bond formation energy ( $\Delta E_{int}$ ) between the interacting fragments is dissected into electrostatic attraction ( $\Delta E_{elstat}$ ), Pauli repulsion ( $\Delta E_{Pauli}$ ), and orbital (covalent) interactions ( $\Delta E_{orb}$ ). The latter term can be divided with the help of the NOCV (natural orbitals for chemical valence) method into pairwise contributions of the different orbitals. The dissociation energy can be computed by considering the energy for the relaxation of the fragments ( $-D_e = \Delta E_{int} + \Delta E_{prep}$ ). Further details are given in the Supporting Information.<sup>[16]</sup>

For the sake of comparison, we have included the  $[(NHCMe_2)_2M]$  derivatives [ $M=Pd$  (**7**),  $Pt$  (**8**)]. The structures (see the Supporting Information, Figure S13) are in good agreement with experimental X-ray data.<sup>[11]</sup> NBO calculations (see the Supporting Information, Table S9) indicate a charge donation ( $Me_2-cAAC \rightarrow M \leftarrow Me_2-cAAC$ ), which gives negative partial charges at the metal of –0.36 (Pd) and –0.32 (Pt) for **3** and

**6**, respectively; whereas the charge donation ( $\text{NHC}^{\text{Me}}\rightarrow\text{M}\leftarrow(\text{NHC}^{\text{Me}})$ ) yields slightly more negatively charged metals;  $-0.46$  and  $-0.48$  for Pd and Pt complexes, respectively.

The NBO data are complemented by the EDA results, which give more detailed information about the nature of the metal-ligand interactions in  $[(\text{Me}_2\text{-cAAC})_2\text{M}]$  [ $\text{M}=\text{Pd}$  (**3**),  $\text{Pt}$  (**6**)] and  $[(\text{NHC}^{\text{Me}})_2\text{M}]$  [ $\text{M}=\text{Pd}$  (**7**),  $\text{Pt}$  (**8**); Table 2].

**Table 2.** EDA-NOCV calculations at the BP86/TZ2P+ level of  $[(\text{Me}_2\text{-cAAC})_2\text{M}]$  ( $\text{M}=\text{Pd}$  (**3**),  $\text{Pt}$  (**6**)) and  $[(\text{NHC}^{\text{Me}})_2\text{M}]$  ( $\text{M}=\text{Pd}$  (**7**),  $\text{Pt}$  (**8**)). Energy values are given in  $\text{kcal mol}^{-1}$ .<sup>[a]</sup>

L	$\text{Me}_2\text{-cAAC}$		$\text{NHC}^{\text{Me}}$	
M	Pd ( <b>3</b> )	Pt ( <b>6</b> )	Pd ( <b>7</b> )	Pt ( <b>8</b> )
$\Delta E_{\text{int}}$	-117.3	-181.7	-109.7	-169.3
$\Delta E_{\text{Pauli}}$	320.7	430.7	300.0	400.0
$\Delta E_{\text{elstat}}$	-296.6 (67.7%)	-405.3 (66.2%)	-282.3 (68.9%)	-382.1 (67.1%)
$\Delta E_{\text{orb}}$	-141.4 (32.3%)	-207.1 (33.8%)	-127.4 (31.1%)	-187.2 (32.9%)
$\Delta E_{\sigma}$	-71.4	-109.4	-74.5	-110.7
$\text{Ms}(\sigma)\leftarrow(\text{L})_2$ <sup>[b]</sup>	(50.5%)	(52.8%)	(58.5%)	(59.1%)
$\Delta E_{\sigma}$	-8.6	-16.0	-8.4	-15.4
$\text{Mp}(\sigma)\leftarrow(\text{L})_2$ <sup>[b]</sup>	(6.1%)	(7.7%)	(6.6%)	(8.2%)
$\Delta E_{\pi\parallel}$	-30.5	-37.1	-18.9	-24.5
$\text{Md}(\pi)\rightarrow(\text{L})_2$ <sup>[b]</sup>	(21.6%)	(17.9%)	(14.8%)	(13.1%)
$\Delta E_{\pi\perp}$	-20.8	-27.5	-16.7	-21.3
$\text{Md}(\pi)\rightarrow(\text{L})_2$ <sup>[b]</sup>	(14.7%)	(13.3%)	(13.1%)	(11.4%)
$\Delta E_{\text{rest}}$	-10.1 (7.1%)	-17.1 (8.3%)	-8.9 (7.0%)	-15.3 (8.2%)
$\Delta E_{\text{prep total}}$	14.0	15.5	5.8	6.2
$-D_e$	-103.3	-166.2	-103.9	-163.1

[a] Unless otherwise stated, the values in parentheses give the percentage contribution to the total attractive interactions  $\Delta E_{\text{elstat}} + \Delta E_{\text{orb}}$ ; [b] the values in parentheses give the percentage contribution to the total orbital interactions  $\Delta E_{\text{orb}}$ .

The EDA data suggest that the intrinsic metal-ligand interactions of the cAAC complexes are slightly higher than those of the NHC adducts. The Pt complexes have, in all cases, significantly stronger bonds than the Pd species. The bond dissociation energies ( $-D_e$ ) follow the same trend as the intrinsic interaction energies and indicate that all complexes are stable. The attractive interaction comes from the ionic term  $\Delta E_{\text{elstat}}$ , which contributes more than 66% to the bonding, whereas the covalent (orbital) term  $\Delta E_{\text{orb}}$  comprises around 34%. The breakdown of the orbital interaction term  $\Delta E_{\text{orb}}$  indicates that the  $\sigma$  donation  $\text{L}\rightarrow\text{M}\leftarrow\text{L}$  has similar strength for  $\text{L}=\text{Me}_2\text{-cAAC}$  and  $\text{L}=\text{NHC}^{\text{Me}}$ , whereas the  $\text{L}\leftarrow\text{M}\rightarrow\text{L}$   $\pi$  back-donation of  $\text{L}=\text{Me}_2\text{-cAAC}$  is clearly stronger than that for  $\text{L}=\text{NHC}^{\text{Me}}$ . The deformation densities are displayed in Figure S14 (see the Supporting Information). The  $\pi$  back-donation in the platinum complex **6** is calculated to be stronger than that in the palladium complex **3**, in agreement with the experimental difference in the C–N distances for **6**·0.5THF and **1**·1·THF that were discussed above.

The cyclic voltammograms (Figure 4) of THF solutions of **1** and **6** containing 0.1 M  $[\text{nBu}_4\text{N}]^+\text{ClO}_4^-$  as electrolyte (CE=Pt; WE=GC; RE=Ag) show a one-electron quasi-reversible oxida-

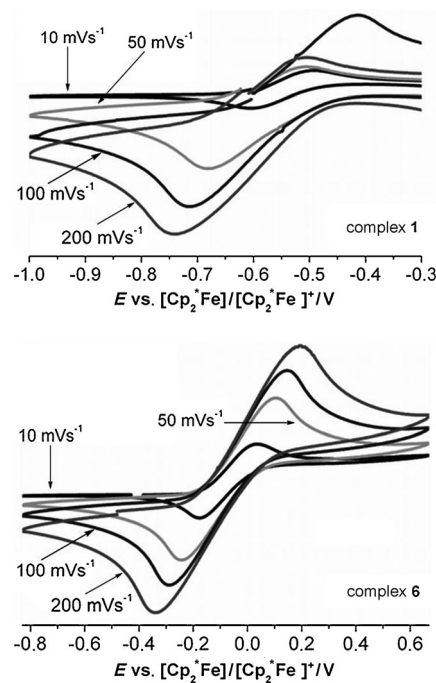
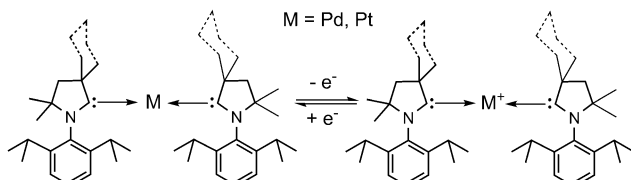


**Figure 4.** Section of cyclic voltammogram of a THF solution of **1** (top) and **6** (bottom) at indicated scan rates. The solution contained 0.1 M  $[\text{nBu}_4\text{N}]^+\text{ClO}_4^-$  as an electrolyte.

tion of  $E_{1/2}=-0.60$  V (Pd; **1**) and  $E_{1/2}=-0.07$  V (Pt; **6**) versus  $[\text{Cp}^*\text{Fe}]/[\text{Cp}^*\text{Fe}]^+$ , indicating the formation of the stable cationic species  $[(\text{cAAC})_2\text{M}]^+$  ( $\text{M}=\text{Pd}, \text{Pt}$ ; Scheme 2). The widening between the anodic and cathodic potentials of cationic complexes suggests slight structural changes. Removal of an electron from the HOMO results in the depletion of electron density on the metal center. The optimized structures of the cations **3**<sup>+</sup> and **6**<sup>+</sup> present small differences with respect to the neutral complexes; longer M–C bond lengths and shorter C–N bond lengths, while the angle C–M–C is almost invariable. Finally,  $(\text{cAAC})_2\text{Pt}$  (**4**–**6**) complexes were further characterized by <sup>195</sup>Pt NMR spectroscopy ( $-4247.07$  (**4**),  $-4333.82$  (**5**),  $-4211.56$  ppm (**6**)). The <sup>195</sup>Pt chemical shift values are in the expected range of previous reports.<sup>[19]</sup> The  $J_{\text{C(cAAC)-Pt}}$  values are 1158.3 (**4**), 1150.7 (**5**), 1144.4 Hz (**6**) while  $J_{\text{NCMe}_2\text{-Pt}}/J_{\text{CCarbeneCMe}_2}$  values are 85.7/105.6 (**4**), 86.2/95.9 (**5**), 88.9/132.7 Hz (**6**).

Zero-valent palladium and platinum complexes are well known as efficient catalysts.<sup>[13b,c,14,16]</sup>  $\pi$ -Accepting ligands have been suggested to be superior for coupling reactions, as supported by the results of theoretical calculations.<sup>[13b,c]</sup> In summary,



**Scheme 2.** Reversible one-electron oxidation of  $[(\text{cAAC})_2\text{M}]$  complexes; ( $\text{M}=\text{Pd}, \text{Pt}$ ).

ry, we have shown that  $\pi$ -accepting cyclic alkyl(amino) carbenes (cAACs) react with tetrakis(triphenylphosphine)palladium(0) and the corresponding platinum(0) precursors to form  $[(\text{cAAC})_2\text{Pd}/\text{Pt}]$  complexes (**1–6**) with two-coordinate Pd or Pt atoms. Sterically less crowded  $\text{Me}_2\text{—cAAC}$  is a more suitable ligand than  $\text{Et}_2\text{—cAAC}$  or  $\text{Cy}\text{—cAAC}$ , with better yields and lower reaction times. These complexes were characterized by NMR spectroscopy, mass spectrometry, and single-crystal X-ray diffraction. The crystals of **1–6** are stable in air for several hours but stable for months under an inert atmosphere at room temperature. The Cy—cAAC and  $\text{Me}_2\text{—cAAC}$  analogues are both thermally stable above  $200^\circ\text{C}$ , whereas the  $\text{Et}_2\text{—cAAC}$  analogues are stable above  $140^\circ\text{C}$ . CV measurements showed that both Pd (**1**) and Pt (**6**) complexes quasi-reversibly undergo one-electron oxidation to produce their corresponding cations  $[(\text{Cy—cAAC})_2\text{Pd}]^+$  and  $[(\text{Me}_2\text{—cAAC})_2\text{Pt}]^+$ .

Interestingly,  $[(\text{cAAC})_2\text{Pd}]$  complexes exhibit crystallochromism, changing color from dark maroon to bright green due to bending of the C-Pd-C bond angle from  $172.75(6)^\circ$  to  $166.94(6)^\circ$ . Both the conformers of this series of complexes (**1**·THF and **1**) are present in solution and can be separated in the solid state by crystallization, either in a freezer at  $-32^\circ\text{C}$  or at room temperature. To our knowledge, this phenomenon is unprecedented for carbene–metal(0) complexes.<sup>[20]</sup>

## Acknowledgements

H.W.R. thanks the Deutsche Forschungsgemeinschaft (DFG RO 224/60-I) for financial support. D.S. thanks the Fonds der Chemischen Industrie for financial support.

**Keywords:** carbenes · crystallochromism · density functional calculations · palladium · platinum

- [1] a) A. J. Arduengo, III, R. L. Harlow, M. Kline, *J. Am. Chem. Soc.* **1991**, *113*, 361–363; b) F. E. Hahn, M. C. Jahnke, *Angew. Chem. Int. Ed.* **2008**, *47*, 3122–3172; *Angew. Chem.* **2008**, *120*, 3166–3216; c) D. Bourissou, O. Guerret, F. P. Gabbaï, G. Bertrand, *Chem. Rev.* **2000**, *100*, 39–91.
- [2] a) M. N. Hopkinson, C. Richter, M. Schedler, F. Glorius, *Nature* **2014**, *510*, 485–496; b) C. D. Martin, M. Soleilhavoup, G. Bertrand, *Chem. Sci.* **2013**, *4*, 3020–3030; c) Y. Wang, G. H. Robinson, *Dalton Trans.* **2012**, *41*, 337–345; d) S. Díez-González, N. Marion, S. P. Nolan, *Chem. Rev.* **2009**, *109*, 3612–3676; e) R. Tonner, G. Heydenrych, G. Frenking, *Chem. Asian J.* **2007**, *2*, 1555–1567.
- [3] R. S. Ghadwal, R. Azhakar, H. W. Roesky, *Acc. Chem. Res.* **2013**, *46*, 444–456.
- [4] a) D. Martin, M. Melaimi, M. Soleilhavoup, G. Bertrand, *Organometallics* **2011**, *30*, 5304–5313; b) D. Martin, Y. Canac, V. Lavallo, G. Bertrand, *J. Am. Chem. Soc.* **2014**, *136*, 5023–5030.
- [5] V. Lavallo, Y. Canac, C. Präsang, B. Donnadieu, G. Bertrand, *Angew. Chem. Int. Ed.* **2005**, *44*, 5705–5709; *Angew. Chem.* **2005**, *117*, 5851–5855.
- [6] a) D. Martin, M. Soleilhavoup, G. Bertrand, *Chem. Sci.* **2011**, *2*, 389–399; b) K. C. Mondal, H. W. Roesky, M. C. Schwarzer, G. Frenking, B. Niepötter, H. Wolf, R. Herbst-Irmer, D. Stalke, *Angew. Chem. Int. Ed.* **2013**, *52*, 2963–2967; *Angew. Chem.* **2013**, *125*, 3036–3040; c) B. Niepötter, R. Herbst-Irmer, D. Kratzert, P. P. Samuel, K. C. Mondal, H. W. Roesky, P. Jerabek, G. Frenking, D. Stalke, *Angew. Chem. Int. Ed.* **2014**, *53*, 2766–2770; *Angew. Chem.* **2014**, *126*, 2806–2811.
- [7] a) R. Kinjo, B. Donnadieu, G. Bertrand, *Angew. Chem. Int. Ed.* **2010**, *49*, 5930–5933; *Angew. Chem.* **2010**, *122*, 6066–6069; b) O. Back, B. Donnadieu, P. Parameswaran, G. Frenking, G. Bertrand, *Nat. Chem.* **2010**, *2*, 369–373; c) O. Back, M. A. Celik, G. Frenking, M. Melaimi, B. Donnadieu, G. Bertrand, *J. Am. Chem. Soc.* **2010**, *132*, 10262–10263; d) R. Kinjo, B. Donnadieu, M. A. Celik, G. Frenking, G. Bertrand, *Science* **2011**, *333*, 610–613; e) D. Martin, C. E. Moore, A. L. Rheingold, G. Bertrand, *Angew. Chem. Int. Ed.* **2013**, *52*, 7014–7017; *Angew. Chem.* **2013**, *125*, 7152–7155; f) V. Lavallo, Y. Canac, B. Donnadieu, W. W. Schoeller, G. Bertrand, *Angew. Chem. Int. Ed.* **2006**, *45*, 3488–3491; *Angew. Chem.* **2006**, *118*, 3568–3571; g) K. C. Mondal, H. W. Roesky, M. C. Schwarzer, G. Frenking, I. Tkach, H. Wolf, D. Kratzert, R. Herbst-Irmer, B. Niepötter, D. Stalke, *Angew. Chem. Int. Ed.* **2013**, *52*, 1801–1805; *Angew. Chem.* **2013**, *125*, 1845–1850; h) K. C. Mondal, H. W. Roesky, A. C. Stückl, F. Ihret, W. Kaim, B. Dittrich, B. Maity, D. Koley, *Angew. Chem. Int. Ed.* **2013**, *52*, 11804–11807; *Angew. Chem.* **2013**, *125*, 12020–12023.
- [8] a) K. C. Mondal, P. P. Samuel, H. W. Roesky, E. Carl, R. Herbst-Irmer, D. Stalke, B. Schwederski, W. Kaim, L. Ungur, L. F. Chibotaru, M. Hermann, G. Frenking, *J. Am. Chem. Soc.* **2014**, *136*, 1770–1773; b) R. Kretschmer, D. A. Ruiz, C. E. Moore, A. L. Rheingold, G. Bertrand, *Angew. Chem. Int. Ed.* **2014**, *53*, 8176–8179; *Angew. Chem.* **2014**, *126*, 8315–8318.
- [9] P. Jerabek, H. W. Roesky, G. Bertrand, G. Frenking, *J. Am. Chem. Soc.* **2014**, *136*, 17123–17135.
- [10] a) M. Melaimi, M. Soleilhavoup, G. Bertrand, *Angew. Chem. Int. Ed.* **2010**, *49*, 8810–8849; *Angew. Chem.* **2010**, *122*, 8992–9032; b) K. C. Mondal, P. P. Samuel, H. W. Roesky, R. R. Aysin, L. A. Leites, S. Neudeck, J. Lübben, B. Dittrich, M. Hermann, G. Frenking, *J. Am. Chem. Soc.* **2014**, *136*, 8919–8922; c) J. Böhnke, H. Braunschweig, W. C. Ewing, C. Hörl, T. Kramer, I. Krummenacher, J. Mies, A. Vargas, *Angew. Chem. Int. Ed.* **2014**, *53*, 9082–9085; *Angew. Chem.* **2014**, *126*, 9228–9231; d) M. Soleilhavoup, G. Bertrand, *Acc. Chem. Res.* **2015**, *48*, 256–266.
- [11] a) A. J. Arduengo, III, S. F. Camper, J. C. Calabrese, F. Davidson, *J. Am. Chem. Soc.* **1994**, *116*, 4391–4394; b) C. W. K. Gstöttmayr, V. P. W. Böhm, E. Herdtweck, M. Grosche, W. A. Herrmann, *Angew. Chem. Int. Ed.* **2002**, *41*, 1363–1365; *Angew. Chem.* **2002**, *114*, 1421–1423.
- [12] a) P. P. Samuel, K. C. Mondal, H. W. Roesky, M. Hermann, G. Frenking, S. Demeshko, F. Meyer, A. C. Stückl, J. H. Christian, N. S. Dalal, L. Ungur, L. F. Chibotaru, K. Pröpper, A. Meents, B. Dittrich, *Angew. Chem. Int. Ed.* **2013**, *52*, 11817–11821; *Angew. Chem.* **2013**, *125*, 12033–12037; b) G. Ung, J. Rittle, M. Soleilhavoup, G. Bertrand, J. C. Peters, *Angew. Chem. Int. Ed.* **2014**, *53*, 8427–8431; *Angew. Chem.* **2014**, *126*, 8567–8571; c) K. C. Mondal, S. Roy, S. De, P. Parameswaran, B. Dittrich, S. Demeshko, F. Ehret, W. Kaim, H. W. Roesky, *Chem. Eur. J.* **2014**, *20*, 11646–11649; d) K. C. Mondal, P. P. Samuel, Y. Li, H. W. Roesky, S. Roy, L. Ackermann, N. S. Sidhu, G. M. Sheldrick, E. Carl, S. Demeshko, S. De, P. Parameswaran, L. Ungur, L. F. Chibotaru, D. M. Andrade, *Eur. J. Inorg. Chem.* **2014**, 818–823; e) D. S. Weinberger, N. A. SK, K. C. Mondal, M. Melaimi, G. Bertrand, A. C. Stückl, H. W. Roesky, B. Dittrich, S. Demeshko, B. Schwederski, W. Kaim, P. Jerabek, G. Frenking, *J. Am. Chem. Soc.* **2014**, *136*, 6235–6238; f) A. P. Singh, P. P. Samuel, H. W. Roesky, M. C. Schwarzer, G. Frenking, N. S. Sidhu, B. Dittrich, *J. Am. Chem. Soc.* **2013**, *135*, 7324–7329.
- [13] a) D. Weinberger, M. Melaimi, C. E. Moore, A. L. Rheingold, G. Frenking, P. Jerabek, G. Bertrand, *Angew. Chem. Int. Ed.* **2013**, *52*, 8964–8967; *Angew. Chem.* **2013**, *125*, 9134–9137; b) A. K. de K. Lewis, S. Caddick, F. G. N. Cloke, N. C. C. Billingham, P. B. Hitchcock, J. Leonard, *J. Am. Chem. Soc.* **2003**, *125*, 10066–10073; c) T. E. Bader, S. D. Walker, J. R. Martinelli, S. L. Buchwald, *J. Am. Chem. Soc.* **2005**, *127*, 4685–4696.
- [14] a) P. L. Arnold, F. G. N. Cloke, T. Geldbach, P. B. Hitchcock, *Organometallics* **1999**, *18*, 3228–3233; b) V. P. W. Böhm, C. W. K. Gstöttmayr, T. Westkamp, W. A. Herrmann, *J. Organomet. Chem.* **2000**, *595*, 186–190; c) S. Caddick, F. G. N. Cloke, G. K. B. Cleatsmith, P. B. Hitchcock, D. McKerrecher, L. R. Titcomb, M. R. V. Williams, *J. Organomet. Chem.* **2001**, *617*–618, 635–639; d) S. Caddick, F. G. N. Cloke, P. B. Hitchcock, J. Leonard, A. K. de K. Lewis, D. McKerrecher, L. R. Titcomb, *Organometallics* **2002**, *21*, 4318–4319; e) K. Arentsen, S. Caddick, F. G. N. Cloke, *Tetrahedron* **2005**, *61*, 9710–9715; f) N. Stylianides, A. A. Danopoulos, D. Pugh, F. Hancock, A. Zanotti-Gerosa, *Organometallics* **2007**, *26*, 5627–5635; g) A. K. de K. Lewis, S. Caddick, O. Esposito, F. G. N. Cloke, P. B. Hitchcock, *Dalton Trans.* **2009**, 7094–7098; h) L. A. Labios, M. D. Millard, A. L. Rheingold, J. S. Figueroa, *J. Am. Chem. Soc.* **2009**, *131*, 11318–11319; i) L. R. Titcomb, S. Caddick, F. G. N. Cloke, D. J. Wilsona, D. McKerrecher, *Chem. Commun.* **2001**, 1388–1389.

- [15] a) J. Bauer, H. Braunschweig, P. Brenner, K. Kraft, K. Radacki, K. Schwab, *Chem. Eur. J.* **2010**, *16*, 11985–11992; b) A. Languérand, S. S. Barnes, G. Bélanger-Chabot, L. Maron, P. Berrouard, P. Audet, F.-G. Fontaine, *Angew. Chem. Int. Ed.* **2009**, *48*, 6695–6698; *Angew. Chem.* **2009**, *121*, 6823–6826; c) G. C. Fortman, N. M. Scott, A. Linden, E. D. Stevens, R. Dorta, S. P. Nolan, *Chem. Commun.* **2010**, *46*, 1050–1052; d) M. Brendel, C. Braun, F. Rominger, P. Hofmann, *Angew. Chem. Int. Ed.* **2014**, *53*, 8741–8745; *Angew. Chem.* **2014**, *126*, 8886–8890.
- [16] For the description of the theoretical methods see the Supporting Information.
- [17] V. Jonas, G. Frenking, M. T. Reetz, *J. Am. Chem. Soc.* **1994**, *116*, 8741–8753.
- [18] a) N. Holzmann, D. Dange, C. Jones, G. Frenking, *Angew. Chem. Int. Ed.* **2013**, *52*, 3004–3008; *Angew. Chem.* **2013**, *125*, 3078–3082; b) G. Frenking, F. M. Bickelhaupt in *The Chemical Bond: Fundamental Aspects of Chemical Bonding* (Eds.: G. Frenking, S. Shaik), Wiley-VCH, Weinheim, **2014**, pp. 121–158; c) M. Chen, Q. Zhang, M. Zhou, D. M. Andrade, G. Frenking, *Angew. Chem.* **2015**, *127*, 126–130; *Angew. Chem. Int. Ed.* **2015**, *54*, 124–128; d) M. von Hopffgarten, G. Frenking, *WIREs Comput. Mol. Sci.* **2012**, *2*, 43–52; e) M. Lein, G. Frenking in *Theory and Applications of Computational Chemistry: The First 40 Years* (Eds.: C. E. Dykstra, G. Frenking, K. S. Kim, G. E. Scuseria), Elsevier, Amsterdam, **2005**, pp. 291–372; f) G. Frenking, K. Wichmann, N. Fröhlich, C. Loschen, M. Lein, J. Frunzke, V. M. Rayón, *Coord. Chem. Rev.* **2003**, *238*–*239*, 55–82.
- [19] B. M. Still, P. G. A. Kumar, J. R. Aldrich-Wright, W. S. Price, *Chem. Soc. Rev.* **2007**, *36*, 665–686.
- [20] O. S. Wenger, *Chem. Rev.* **2013**, *113*, 3686–3733.

---

Received: February 24, 2015

Published online on ■■■, 0000

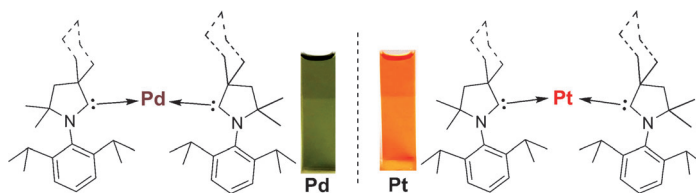
---

## COMMUNICATION

**Carbene Complexes**

S. Roy, K. C. Mondal, J. Meyer,  
B. Niepötter, C. Köhler, R. Herbst-Irmer,  
D. Stalke,\* B. Dittrich, D. M. Andrade,  
G. Frenking,\* H. W. Roesky\*

■ ■ - ■ ■

**Synthesis, Characterization, and Theoretical Investigation of Two-Coordinate Palladium(0) and Platinum(0) Complexes Utilizing  $\pi$ -Accepting Carbenes**

**Bent out of shape:**  $\pi$ -Accepting cyclic alkyl(amino) carbenes were employed for the preparation of two-coordinate, bent palladium(0) and platinum(0) complexes. The palladium complex exhibits crystallochromism (from maroon to

green) due to controlled bending of the C-Pd-C bond angle by approximately  $6^\circ$  during elimination of a lattice solvent molecule. The bonding and stability of these complexes are studied by theoretical calculations. ■ ■ ■ ■